

# Exploring Photoproduction with the GlueX Experiment

Matthew Shepherd<sup>1,\*</sup>

<sup>1</sup>Indiana University, Bloomington, IN 47405, USA

**Abstract.** The GlueX experiment at Jefferson Lab (Newport News, VA USA) is designed to explore the spectrum of mesons up to about 3 GeV. We present results on the production of light-quark resonances with linearly polarized photons. These results enhance our understanding of photoproduction mechanisms, which is valuable in subsequent searches for exotic hybrid mesons. Measurements of the  $J/\psi$  photoproduction cross section at threshold are also presented.

## 1 Introduction

An outstanding puzzle in our study of strong interactions is understanding how the spectrum of mesons arises from Quantum Chromodynamics. There is a growing body of evidence that QCD generates mesons and baryons beyond quark-antiquark and three-quark configurations. In addition, theoretical calculations of the spectrum of mesons predict states with gluonic degrees of freedom that arise from the gluon-gluon interaction in QCD. A key objective of the GlueX experiment is search for these hybrid mesons in the light quark sector using linearly polarized photon beams, which provide sensitivity to production dynamics. We present a collection of initial results that are useful for developing theoretical and experimental tools for the study of meson photoproduction and ultimately the search for hybrid mesons.

## 2 The GlueX Experiment

The GlueX experiment is designed to explore both production and decay of hadronic resonances. The linearly polarized photon beam, which provides access to experimental observables related to production mechanisms, is derived through coherent bremsstrahlung radiation of the 12 GeV electron beam from Jefferson Lab's Continuous Electron Beam Accelerator Facility (CEBAF) on a thin diamond radiator. The linearly polarized photon beam impinges on a liquid hydrogen (proton) target and the reaction products are detected by the GlueX detector, which has a large acceptance for both charged particles and photons. All results presented in these proceedings rely on exclusive reconstruction of the full reaction to suppress backgrounds. A detailed discussion of the apparatus can be found in Ref. [1].

The photon beam, whose energy and polarization is independently measured with beam-line instrumentation, has a peak polarization of about 35% in the region  $8.2 < E_\gamma$  [GeV]  $< 8.8$ . If one considers only the portion of the beam from that energy region, the photon flux on target peaked at about  $5 \times 10^7$   $\gamma$ /s and the total integrated luminosity on a proton target collected by GlueX through calendar year 2020 is about  $250 \text{ pb}^{-1}$ . For comparison, the  $\rho$  meson cross section is about  $10 \mu\text{b}$ , and resonances like the  $a_2$  have cross sections around tens to hundreds of nanobarns.

---

\*e-mail: mashephe@indiana.edu

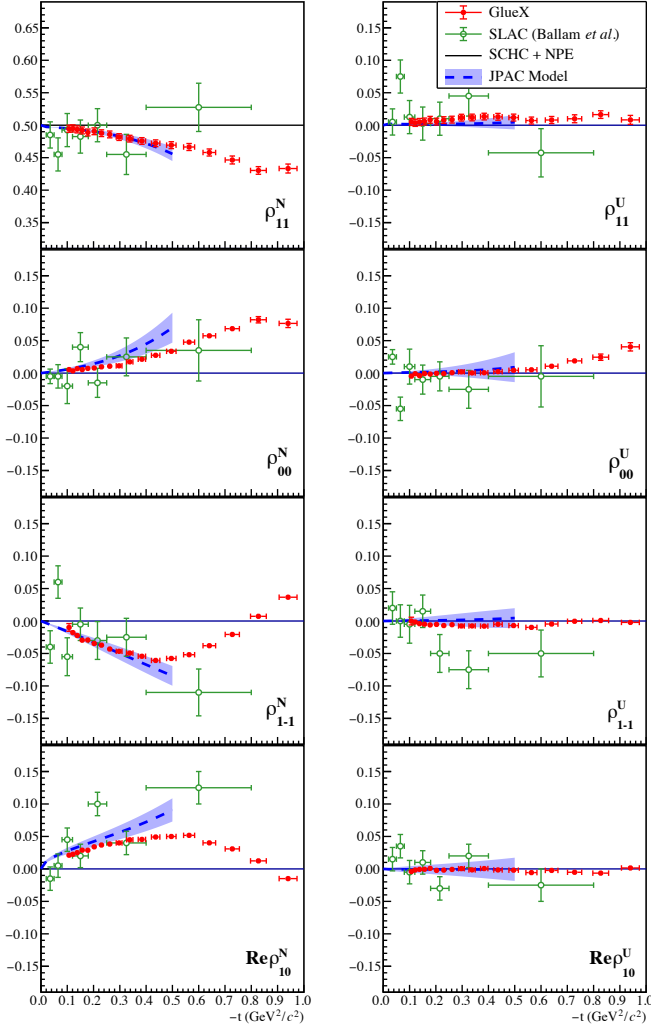


**Figure 1.** The spin-density matrix elements for  $\rho$  meson production are separated into natural parity exchange (left column) and unnatural parity exchange (right column). The existing data from SLAC [5] are shown along with the GlueX results. The data are all compared with a model calculation by the Joint Physics Analysis Center (JPAC) [6]. The limit of pure  $s$ -channel helicity conservation and natural parity exchange is given by the horizontal black lines.

### 3 Spin-Density Matrix Elements for $\rho$ Meson Production

An early goal of the GlueX experiment is to develop an understanding of how to model the photoproduction of meson systems. At beam energies relevant for the GlueX environment, the production of mesons is often modelled as a  $t$ -channel exchange of a virtual particle (a “Reggeon”) with the target. A feature of using linearly polarized photon beams to produce mesons is that it allows access to the naturality of the Reggeon. (Natural parity is defined  $P = (-1)^J$ , whereas unnatural parity is the opposite.) In the production of spinless mesons, the angular distribution of the production plane with respect to linear polarization can be used to extract what is known as the beam asymmetry ( $\Sigma$ ). Early results from GlueX showed the dominance of natural parity exchange [2], except at low momentum transfer ( $t$ ) when pion exchange is allowed [3].

For the production of a vector resonance like the  $\rho^0$ , which decays to  $\pi^+\pi^-$ , the production and polarization of the  $\rho$  can be characterized by a set of spin-density matrix elements (SDMEs)  $\rho(\rho^0)_{ij}^k$ , which are connected to the initial photon spin-density matrix  $\rho(\gamma)$  by a

transition amplitude  $T$ :  $\rho(\rho^0) = T\rho(\gamma)T^*$  [4]. These SDMEs convey not only the quantity of natural and unnatural exchange with the target, but also the transfer of polarization from the incoming polarized photon to the outgoing  $\rho$  resonance. At very low momentum transfer,  $\rho$  production should proceed through  $s$ -channel helicity conserving natural parity exchange (SCHC-NPE), *i.e.*, the  $\rho$  exchanges a particle that has vacuum quantum numbers with the target and emerges with same polarization as the incident photon. As  $|t|$  increases the interaction is expected to deviate from this simplistic picture.

The SDMEs are measured in each region of  $|t|$  by performing a fit of three-dimensional intensity function to the data, where the three relevant angles are the angle that describes the  $\rho$  production with respect to the beam polarization and the two angles that describe the decay of the  $\rho$  and hence encode the  $\rho$  polarization. In the high energy limit, linear combinations of the SDMEs can be used to isolate the natural and unnatural parity exchange components [4], specifically  $\rho_{ik}^{\text{N,U}} = (\rho_{ik}^0 \mp (-1)^i \rho_{-ik}^1)/2$ . The evolution of these SDMEs as a function of  $|t|$  is shown in Fig. 1. For all values of  $t$  the natural parity exchange process dominates over unnatural parity exchange. The deviation from SCHC ( $\rho_{11}^N = \frac{1}{2}$ ) is due to natural parity exchange amplitudes that increase in magnitude with momentum transfer. See Ref. [7] for additional details.

## 4 The Search for Hybrid Mesons

The gluon self-interaction in QCD naively should permit construction of hybrid mesons with gluonic degrees of freedom:  $q\bar{q}g$ . Calculations of the spectrum of light mesons in QCD [8] reveal a rich pattern of states beyond the traditional  $q\bar{q}$  states that have an operator overlap consistent with a hybrid meson interpretation. A striking experimental signature of hybrids is that some of them have exotic  $J^{PC}$ . To date, the best evidence for the existence of hybrid mesons comes from an analysis of COMPASS data on pion production of  $\eta\pi$  and  $\eta'\pi$  [9, 10]. (This work was subsequently extended to include data from Crystal Barrel [11].) The data are consistent with a broad isovector exotic  $J^{PC} = 1^{-+}$  resonance denoted  $\pi_1(1600)$  that couples to both  $\eta\pi$  and  $\eta'\pi$ . While the evidence for this state is strong, one really desires the identification of multiple members of a spectrum of hybrid mesons to understand the role of gluonic degrees of freedom in the hadron spectrum. Further progress towards this goal was made by the BESIII Collaboration who observed a candidate for the exotic  $\eta_1$  or  $\eta'_1$  [12]. An initial target of the GlueX Collaboration is to use photoproduction to confirm the existence of the  $\pi_1(1600)$  and, if observed, study its production mechanisms.

### 4.1 Upper Limits on the $\pi_1(1600)$ Photoproduction Cross Section

In contrast to spinless pion beams, the beam photon can be pictured as a spin-one virtual vector meson. The alignment of quark spins in such states was suggested by some models as a reason for enhanced exotic hybrid cross sections in photoproduction – the  $\pi_1(1600)$  is thought to be the exotic member of a triplet of hybrid states ( $0^{-+}$ ,  $1^{-+}$ , and  $2^{-+}$ ) all with  $S_{q\bar{q}} = 1$ . A challenge with exploring the hypothesis of enhanced photoproduction cross sections of hybrids is that one is experimentally sensitive to the product of production and decay couplings of states. Therefore, it is often difficult to learn about the production cross section from a single measurement. In recent years, calculations of partial widths of exotic hybrid resonances have been performed using Lattice QCD [13]. According to these calculations the dominant decay mode of the  $\pi_1(1600)$  is  $b_1\pi$ . The presence of a single dominant decay mode in the calculation provides a lower limit for the decay coupling and hence the ability to set an upper limit on the production cross section of  $\pi_1(1600)$  using data from GlueX.

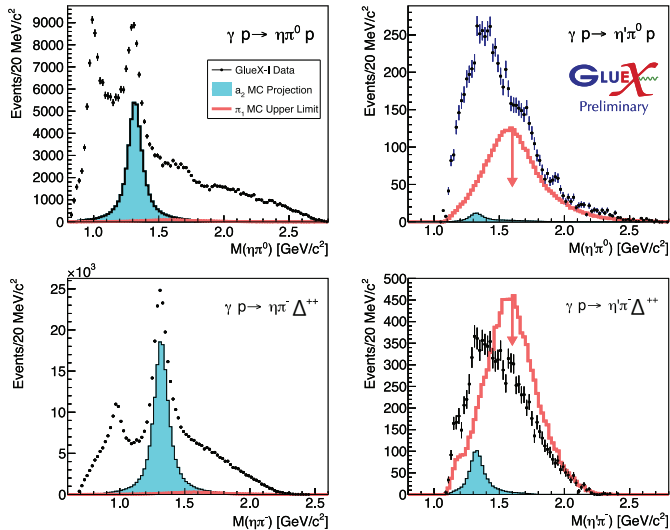


**Figure 2.** Invariant mass spectra for the  $\eta\pi$  (left) and  $\eta'\pi$  (right) systems produced in neutral-exchange recoil proton reaction (upper) and charge-exchange recoil  $\Delta^{++}$  reaction (lower). The projected size of the  $a_2^{-0}$  signal is shown, using branching ratios from the PDG. The red curves show upper limits on the contribution of exotic  $\pi_1$  to the spectra.

Most importantly, this upper limit, coupled again with Lattice QCD calculations of branching ratios, can be used to guide the search for exotic hybrid mesons to the most sensitive reactions.

To obtain upper limits on  $\sigma(\gamma p \rightarrow \pi_1^- \Delta^{++})$  and  $\sigma(\gamma p \rightarrow \pi_1^0 p)$  we first note that the predicted dominant  $b_1\pi$  decay mode of the  $\pi_1$  will produce the final state  $\omega\pi\pi$ . Using GlueX data, we reconstruct the reactions  $\gamma p \rightarrow \omega\pi^+\pi^- p$  and  $\gamma p \rightarrow \omega\pi^0\pi^0 p$  and use isospin relations to isolate the cross section for  $\gamma p \rightarrow (\omega\pi\pi)_{I=1} p$  where we might expect to observe the  $\pi_1^0$  as a peak in the  $\omega\pi\pi$  mass spectrum. In addition, we analyze the isospin-one cross section  $\gamma p \rightarrow (\omega\pi\pi)^- \Delta^{++}$ . No distinct  $\pi_1$  peak appears in either spectrum but assuming the  $\pi_1$  saturates the spectra provides an upper limit for the cross section. Quantitatively, the upper limit for  $\pi_1^-$  photoproduction cross section is at the level of the  $a_2(1320)^-$  cross section. A similar result is obtained for the  $\pi_1^0$  compared to the  $a_2(1320)^0$  cross section. These results suggest the exotic  $\pi_1$  photoproduction cross section is not significantly enhanced with respect to the conventional  $a_2$  meson.

Equally as important, the results, again coupled with LQCD calculations of branching ratios, allow one to set limits on the contribution of the  $\pi_1$  to various spectra. These *upper limits* are shown by the red curves in Fig. 2. Our results exclude a large contribution of the exotic amplitude to the  $\eta\pi$  mass spectrum. However, a large contribution to the  $\eta'\pi^{-0}$  mass spectra is not excluded, and consequently these reactions provide the best sensitivity in a search for the  $\pi_1(1600)$  in photoproduction. Using measured branching ratios from the Particle Data Group, we can also predict the  $a_2$  contribution to each spectrum. Enhancements at the  $a_2$  mass in the data are evident in all spectra. An understanding of conventional  $a_2$  production and polarization is essential as it will act as both a standard candle and interferometer in the search for the exotic  $\pi_1$ .

## 4.2 Photoproduction of $a_2(1320)$

As shown in Fig. 2, the  $a_2(1320)$  is clearly visible as a peak in both the  $\eta\pi^-$  and  $\eta\pi^0$  spectra. In order to facilitate the search for exotic mesons in  $\eta'\pi$ , where the  $a_2$  is comparatively smaller, we need to use the  $\eta\pi$  channels to constrain our knowledge of the  $a_2$ . In the case of  $\gamma p \rightarrow a_2^0 p$  there are ten different amplitudes that provide a description of the production:  $(2J+1)$  possible projections of the  $a_2$  spin times two choices of reflectivity  $\epsilon$ , which, in the high-energy limit,

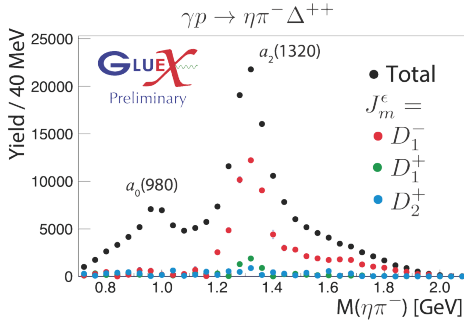


**Figure 3.** The  $\eta\pi^-$  mass spectrum (black points) in the reaction  $\gamma p \rightarrow \eta\pi^- \Delta^{++}$  for  $0.1 < |t|$  [GeV]  $< 0.3$ . The colored points show the result of an amplitude analysis in bins of  $\eta\pi^-$ , where the amplitudes for spin  $J$ , spin-projection  $m$ , and reflectivity  $\epsilon$  are denoted by  $J_m^\epsilon$ .

corresponds to production by natural ( $\epsilon = +$ ) and unnatural ( $\epsilon = -$ ) exchange [14]. At low momentum transfer to the target, the  $a_2^0$  is produced dominantly by natural parity exchange in an  $m = 2$  state denoted  $D_2^+$  (see Ref. [15] for details). Interestingly, a similar helicity structure is also observed in two-photon production of the  $a_2$  [16]. Figure 3 shows the dominant  $D$ -wave amplitudes in the  $\eta\pi^-$  system at low momentum transfer to the target. In addition to the  $a_2(1320)^-$  additional intensity in the  $D$ -wave at higher mass, consistent with the  $a_2'$ , is observed. In contrast to the  $a_2^0$ , the  $a_2^-$  is produced dominantly in the  $D_1^-$  amplitude, which is consistent with a pion exchange process where the  $a_2$  emerges with a polarization that matches the incident beam.

## 5 Photoproduction of $J/\psi$ at Threshold

Measuring the total cross section ( $\sigma$ ) and differential cross section ( $d\sigma/dt$ ) of  $\gamma p \rightarrow J/\psi p$  as a function of beam energy  $E_\gamma$  provides access to a variety of topics. One model for the production process involves conversion of the photon to the  $c\bar{c}$  system via the exchange of high-momentum gluons with the proton. In this picture, the dependence of the cross section on momentum transfer to the proton gives access to the gluonic form-factors of the proton [17]. On the topic of hadron spectroscopy, it is interesting to look for peaks in the cross section as a function of energy. The LHCb collaboration has reported several candidates for pentaquark resonances that couple to  $J/\psi p$  [18]. Naively, one would expect to excite such resonances in photon-proton collisions at of the appropriate energy.

Experimentally, the  $J/\psi$  is detected through its  $e^+e^-$  decay mode, which leaves a unique signature of two high-energy electromagnetic showers in the detector. The recent GlueX measurements [19] for the production cross section of  $J/\psi$  as a function of beam energy are shown in Fig. 4. These measurements reveal an interesting cusp-like structure in the energy dependence of the cross section that coincides with thresholds for production of  $\Lambda_c \bar{D}$  and  $\Lambda_c D^*$ . Additional theoretical work and more precise measurements, especially those with polarization observables, are needed to understand nature of these structures, which may be evidence of resonances or other effects that have implications on the ability to interpret the data in the context of proton gluonic form factors [22].

## 6 Summary and Acknowledgements

In summary, a collection of results from the initial running of the GlueX experiment have been presented. Measurements of  $\rho$  spin-density matrix elements and the properties of  $a_2$  production aid in refinement of photoproduction models. Upper limits on  $\pi_1$  photoproduction cross sections coupled with Lattice QCD results guide the search for exotic mesons. A study

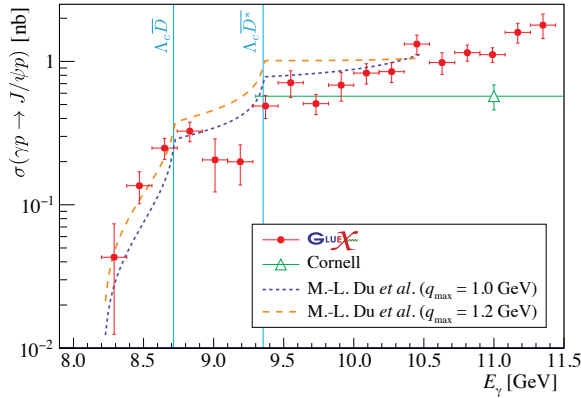


**Figure 4.** The  $J/\psi$  photoproduction cross section as a function of photon beam energy measured by GlueX (red points). A previous measurement from Cornell [20] is shown in the green point. The dashed and dotted lines show cross section calculation for a model that includes the effects of open charm thresholds  $\Lambda_c \bar{D}$  and  $\Lambda_c \bar{D}^*$  [21].

of  $J/\psi$  production provides an opportunity to enhance our understanding of the proton and constrain properties of candidates for pentaquarks containing  $c\bar{c}$ .

I would like to thank my colleagues in the GlueX Collaboration and the MESON 2023 organizers for the opportunity to present these results. This work was funded in part by the US Department of Energy Office of Nuclear Physics under grant DE-FG02-05ER41374.

## References

- [1] S. Adhikari *et al.* [GlueX Collaboration], Nucl. Instrum. Meth. **A987**, 164807 (2021).
- [2] S. Adhikari *et al.* [GlueX Collaboration], Phys. Rev. C **100**, 052201 (2019).
- [3] S. Adhikari *et al.* [GlueX Collaboraiton], Phys. Rev. C **103**, L022201 (2021).
- [4] K. Schilling, P. Seyboth, and G.E. Wolf, Nucl. Phys. B **15**, 397 (1970).
- [5] J. Ballam *et al.*, Phys. Rev. D **5**, 545 (1972).
- [6] V. Mathieu *et al.* [JPAC Collaboration], Phys. Rev. D **97**, 094003 (2018).
- [7] S. Adhikari *et al.* [GlueX Collaboration], to be published in Phys. Rev. C (arXiv:230509047).
- [8] J. J. Dudek *et al.* [Hadron Spectrum Collaboration], Phys. Rev. D **88**, 094505 (2013).
- [9] C. Adolph *et al.* [COMPASS Collaboration], Phys. Lett. B **740**, 303 (2015).
- [10] A. Rodas *et al.* [JPAC Collaboration], Phys. Rev. Lett. **122**, 042002 (2019).
- [11] B. Kopf *et al.*, Eur. Phys. J. C **81**, 1056 (2021).
- [12] M. Ablikim *et al.* [BESIII Collaboration], Phys. Rev. Lett. **129**, 192002 (2022).
- [13] A. Woss *et al.*, Phys. Rev. D **103**, 054502 (2021).
- [14] V. Mathieu *et al.* [JPAC Collaboration], Phys. Rev. D **100**, 054017 (2019).
- [15] M. Albrecht, Proceedings of HADRON 2023, to be published in Il Nuovo Cimento.
- [16] S. Uehara *et al.* [Belle Collaboration], Phys. Rev. D **80**, 032001 (2009).
- [17] L. Frankfurt and M. Strickman, Phys. Rev. D **66**, 031502(R) (2002).
- [18] R. Aaij *et al.* [LHCb Collaboration], Phys.Rev.Lett. **122**, 222001 (2019).
- [19] S. Adhikari *et al.* [GlueX Collaboration], Phys. Rev. C **108**, 025201 (2023).
- [20] B. Gittelman *et al.*, Phys. Rev. Lett. **35**, 1616 (1975).
- [21] M.-L. Du, *et al.*, Eur. Phys. J C **80**, 1053 (2020).
- [22] D. Winney *et al.* [JPAC Collaboration], Phys. Rev. D **108**, 054018 (2023).